


MINI-SYMPOSIUM : RECENT ADVANCES IN NEUROIMAGING IN MULTIPLE SCLEROSIS, AND THEIR NEUROPATHOLOGICAL SIGNIFICANCE

Myelin water imaging to detect demyelination and remyelination and its validation in pathology

Cornelia Laule^{1,2,3,4}  and G.R. Wayne Moore^{2,4,5}

¹ Radiology, University of British Columbia, Vancouver, BC Canada.

² Pathology & Laboratory Medicine, University of British Columbia, Vancouver, BC Canada.

³ Physics & Astronomy, University of British Columbia, Vancouver, BC Canada.

⁴ International Collaboration on Repair Discoveries (ICORD), University of British Columbia, Vancouver, BC Canada.

⁵ Medicine (Neurology), University of British Columbia, Vancouver, BC Canada.

Keywords

diffusely abnormal white matter, magnetic resonance imaging, multiple sclerosis, myelin, normal appearing white matter, pathology

Corresponding author:

Cornelia Laule and Wayne Moore,
International Collaboration on Repair
Discoveries (ICORD), 818 West 10th
Avenue, Vancouver, BC, Canada V5Z 1M9
(E-mail: corree@physics.ubc.ca;
wmoore@icord.org)

Received 4 July 2018

Accepted 9 July 2018

Published Online Article Accepted

00 Month 2018

doi:10.1111/bpa.12645

Abstract

Damage to myelin is a key feature of multiple sclerosis (MS) pathology. Magnetic resonance imaging (MRI) has revolutionized our ability to detect and monitor MS pathology *in vivo*. Proton density, T₁ and T₂ can provide *qualitative* contrast weightings that yield superb *in vivo* visualization of central nervous system tissue and have proved invaluable as diagnostic and patient management tools in MS. However, standard clinical MR methods are not specific to the types of tissue damage they visualize, and they cannot detect subtle abnormalities in tissue that appears otherwise normal on conventional MRIs. Myelin water imaging is an MR method that provides *in vivo* measurement of myelin. Histological validation work in both human brain and spinal cord tissue demonstrates a strong correlation between myelin water and staining for myelin, validating myelin water as a marker for myelin. Myelin water varies throughout the brain and spinal cord in healthy controls, and shows good intra- and inter-site reproducibility. MS plaques show variably decreased myelin water fraction, with older lesions demonstrating the greatest myelin loss. Longitudinal study of myelin water can provide insights into the dynamics of demyelination and remyelination in plaques. Normal appearing brain and spinal cord tissues show reduced myelin water, an abnormality which becomes progressively more evident over a timescale of years. Diffusely abnormal white matter, which is evident in 20%–25% of MS patients, also shows reduced myelin water both *in vivo* and postmortem, and appears to originate from a primary lipid abnormality with relative preservation of myelin proteins. Active research is ongoing in the quest to refine our ability to image myelin and its perturbations in MS and other disorders of the myelin sheath.

MYELIN IN MULTIPLE SCLEROSIS

The most obvious pathologic feature of multiple sclerosis (MS) are multiple white matter plaques, characterized by demyelination with varying degrees of remyelination, inflammation, and axonal loss (54,95,110,131,133). As is true of all pathologic processes in the central nervous system (CNS) MS plaques also show gliosis, comprised of astrocytes ranging in morphology, depending on the inflammatory demyelination activity of the lesion, from marked acute reactive hyperplastic forms to chronic fibrillary gliosis, the latter imparting the “sclerotic” texture which is responsible for the name of this disorder (110). Subsequently, it was recognized that demyelinated plaques also occur in cortical (13,59,156) and deep gray matter (53,56,181). However, from the very first descriptions of the pathology of MS

(17,18,21,22,26), the white matter demyelinated plaque has been the most prominently emphasized and consistent feature of MS, making it the prototypic “demyelinating disease.” While it is becoming increasingly obvious that axonal damage occurs in MS (41,167) and the relentless degeneration of axons is probably the most important contributor to clinical progression (164), the overwhelming majority of MS plaques manifest a greater degree of loss of myelin than axons. This would indicate that demyelination, which manifests clinically as focal deficits resulting from conduction block of the action potential (152), must be an important primary pathogenic event in MS.

Thus, early on in the 1980s when magnetic resonance imaging (MRI) was first introduced and it became clear that this was an exquisitely sensitive tool for the

demonstration of MS plaques *in vivo* (127,160), one of the main objectives was to determine the MRI features that could be attributable to each of the histopathologic features of MS, but most particularly demyelination, which at that time was the major feature thought to be responsible for MS symptomatology. However, it soon became apparent that routine clinical MR imaging did not correlate with any specific histopathologic feature and the MR image was probably a composite that resulted from the contribution of any number of histologic features in a given plaque (109). Thus, demyelination (35), macrophage infiltration (115), vascular permeability (117), edema (125), gliosis (159), could all either individually or in orchestration, produce the images seen on conventional clinical MRI.

MAGNETIC RESONANCE AND MYELIN WATER IMAGING

Water as the dominant source of contrast in MRI

MRI has revolutionized our ability to detect and monitor MS pathology *in vivo*. The most common type of MR is known as “proton” MR which is sensitive to signal from all of the protons or hydrogen atoms in tissue. The overwhelming majority of the signal measured by proton MRI of the brain and spinal cord originates from hydrogen in water molecules. The properties of the hydrogen govern the three fundamental contrast mechanisms in MRI: [1] **proton density** (proportional to water content) (165); [2] **T₁ relaxation** (influenced heavily by water content as well as the presence of other tissue constituents such as iron and myelin, and factors including field strength, temperature, and MR magnetization exchange processes (40,47,138,162)) and [3] **T₂ relaxation** (related to water content, the nature of the tissue microstructure, iron, pH, and MR magnetization exchange).

Use and limitations of conventional MRI

Proton density, T₁ and T₂ can provide *qualitative* contrast weightings that yield superb *in vivo* visualization of CNS tissue and have proved invaluable as diagnostic and patient management tools in MS (94,140). Conventional MR techniques play a crucial role in the clinic, and while there is some evidence that certain aspects of image contrast are related to severity of damage (ie, permanent black holes evident on T₁-weighted imaging are felt to be indicative of parenchymal destruction (169)), standard clinical MR methods are not specific to the types of tissue damage they visualize, and they cannot detect subtle abnormalities in tissue. Thus, more *quantitative* approaches have evolved that focus on measuring specific tissue properties (165). For example, magnetic resonance spectroscopy (MRS) offered some histopathologic correlative specificity as it demonstrates the presence of molecules that serve as specific markers for various CNS cell types. Of particular note is N-acetyl aspartate (NAA), a marker of axons and coupling between neurons/oligodendrocytes (12,120), which correlates with

axonal loss in MS plaques (8). With respect to myelin specificity, an important scientific breakthrough was the discovery of the short-T₂ component, or myelin water fraction.

Myelin water imaging

Given the important role myelin damage and loss plays in MS, there has been much interest in the development, validation, and implementation of MR techniques for imaging myelination. While several quantitative methods have been proposed as being sensitive to myelin (81), in this review we shall focus primarily on one of these techniques—*myelin water imaging*. The concept of myelin water imaging is based on the fact that, while the entire MR signal is from protons in water molecules, individual water molecules can experience very different microscopic environments, depending on their physical location. If the total MRI signal comes from water in different non-exchanging environments, the resulting T₂ relaxation decay curve of that signal is a sum of exponential decays with amplitudes proportional to the relative amounts of water in each environment. Conceptually, the physical size of the reservoir is a key factor in determining the T₂ relaxation time of the water within that reservoir—water in tightly confined spaces will have a shorter T₂ than water in less tightly confined spaces. For the case of heterogeneous CNS tissue, the T₂ decay can be separated into signal from water trapped in the restricted water reservoir between myelin bilayers (myelin water, Figure 1, T₂ time between 10 and 20 ms), intra/extracellular water (T₂~80–100 ms), additional longer T₂ components seen in some neurological diseases including MS (T₂ ~200–800 ms), and CSF (T₂ of ~2000 ms) (82,84,97,151,189). The T₂ decay curve can then be separated into its exponential components and expressed as a plot of signal amplitude vs. T₂ time, also known as a T₂ distribution (Figure 2) (188). From the T₂ distribution the myelin water fraction (MWF) is defined as the ratio of the area in the T₂ distribution due to myelin water (<40 ms for humans *in vivo* at 1.5T and 3T, <30 ms for formalin-fixed tissue at 1.5T, and <20 ms at 7T) to the area of the entire T₂ distribution. MWF can be visually presented as a myelin water image (Figure 3,4,5,6, 73 to 7).

Myelin water in CNS white matter was first observed in a cat model in 1991 (102). The first human *in vivo* myelin water measurements in the mid-1990s were slow to acquire and produced only a single brain slice in 25 minutes (97); today it is possible to collect whole brain MWF images in less than 5 minutes (118). At least four different approaches to myelin water imaging have now been explored; for a comprehensive technical overview the reader is pointed to a recent review by Alonso-Ortiz *et al* (6). The pioneering, most common, and still considered to be the “gold-standard” approach to myelin water imaging uses a Carr–Purcell–Meiboom–Gill (CPMG) **multi-echo spin echo** data acquisition strategy (97,130,193). Variations on the CPMG method in recent years have resulted in significantly faster imaging times (118,119,122,123,130). Traditional analysis of the T₂ decay used a non-negative least squares (NNLS) method which makes no *a priori* assumptions about the

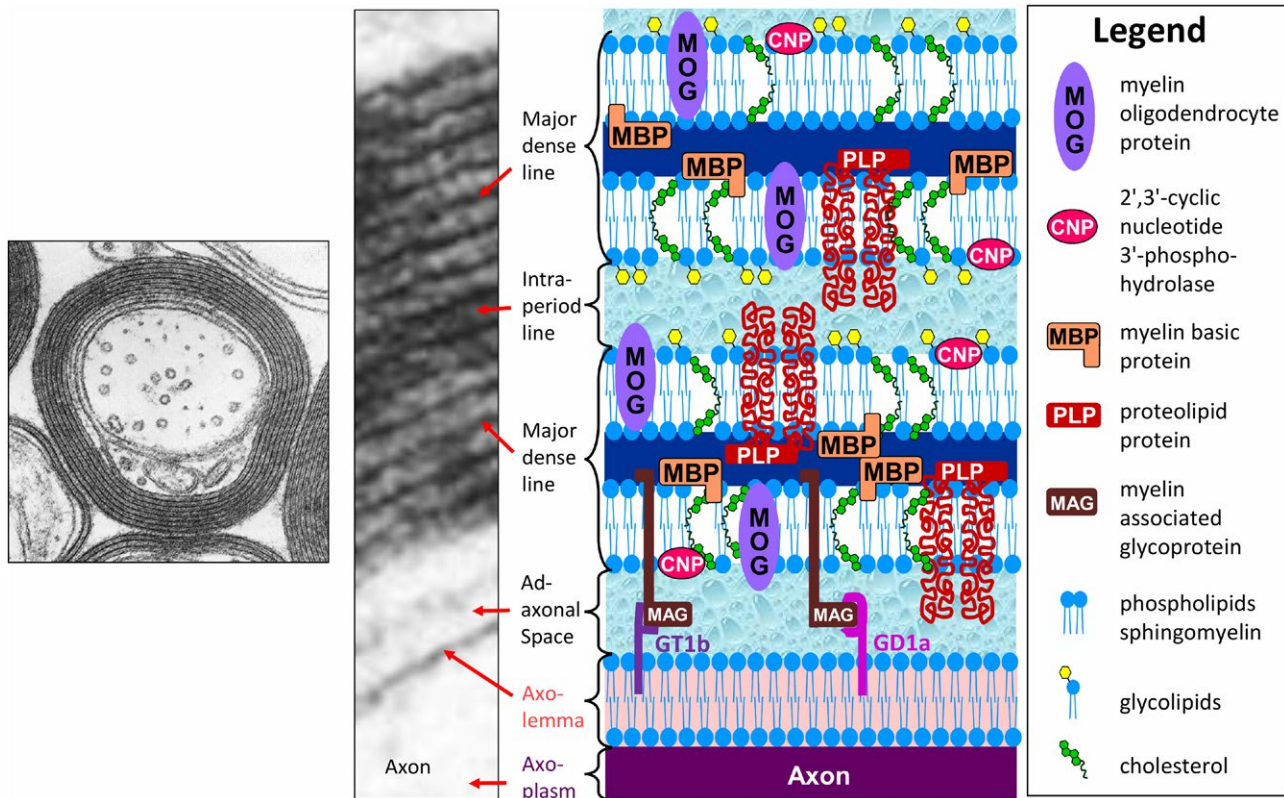


Figure 1. Electron micrograph of myelinated central nervous system (CNS) tissue at low and high magnifications (low magnification (left), adapted from Figure 4–7, originally by Dr. W.T. Norton and Dr. C. S. Raine in Morell P, Quarles RH, Myelin formation, structure, and biochemistry. In Siegel GJ, Agranoff BW, Albers RW, Fisher SK, Uhler MD (editors) Basic Neurochemistry. 6th Edition; 1999. Philadelphia: Lippincott-Raven; ISBN 0-397-51820-X with permission; high magnification (middle) with permission; high magnification (middle) (adapted from Peters A, Palay SL, Webster H deF. Fine Structure of the Nervous System: The Cells and Their Processes. 1st edition; 1970; page 89, Figure 33, New York: Paul B. Hoeber Inc, with permission from Dr. Alan Peters] depicting the major dense line, which represents the fusion of the cytoplasmic aspects of the oligodendrocyte cell membrane, and the intraperiod line, a potential extracellular space formed by the apposition of the extracellular faces of

adjacent oligodendrocyte cell membranes. As shown in the accompanying schematic, the intraperiod line forms a restricted water reservoir, and, thus, is thought to give rise to the short- T_2 component, the signal of which can be displayed anatomically as the myelin water map (see Figure 3, 4, 5, and 6). The oligodendrocyte cell membrane is a bilayer of lipids in which are embedded the major myelin proteins, which include myelin basic protein (MBP), proteolipid protein (PLP), 2',3'-cyclic nucleotide 3'-phosphodiesterase (CNP), myelin oligodendrocyte protein (MOG), and myelin-associated glycoprotein (MAG). Note, however, that on the inner aspect of the myelin sheath MAG is restricted to the membrane adjacent to the adaxonal space, which it spans to bind the myelin sheath to its axolemmal ganglioside receptors, GD1a and GT1b. The exact position of some of the components of myelin shown in this schematic has not been determined.

number of water environments (129,188), although other approaches also exist (2,52,69,70,134,147,157). Several groups have obtained myelin water images from **gradient echo T_2^*** decay curve measurement which examines the echo train derived by magnetic field gradient reversals (32,89,113,142) and measurement of multiple **T_1 relaxation** components to isolate myelin water has also been used (72,124). Finally, the **mcDESPOT** (multicomponent driven equilibrium single pulse observation of T_1 and T_2) method (29) which uses multiple flip angles to examine signal changes of two fast gradient echo imaging sequences to enable demonstration of the myelin water and intra/extracellular water components in CNS tissue has also been used. mcDESPOT is fundamentally different from myelin water imaging techniques which are derived from T_2 , T_2^* , or T_1 decay curves.

VALIDATION OF MYELIN WATER IMAGING

MRI-histology studies of myelin water imaging have focused almost exclusively on validation of the multi-echo spin-echo approach to data acquisition. The myelin water signal is present both shortly after death *in situ* and upon tissue fixation with formalin, and the shape of the T_2 distribution from formalin fixed CNS tissue is qualitatively similar to that from *in vivo*, albeit with shorter T_2 s, (Figure 2) (77), making MRI-pathology correlation studies possible. One of the earliest correlation studies conducted at 1.5T in 2000 showed that the anatomic distribution of the short- T_2 component matched the distribution of myelin and its absence correlated with the absence of myelin in plaques

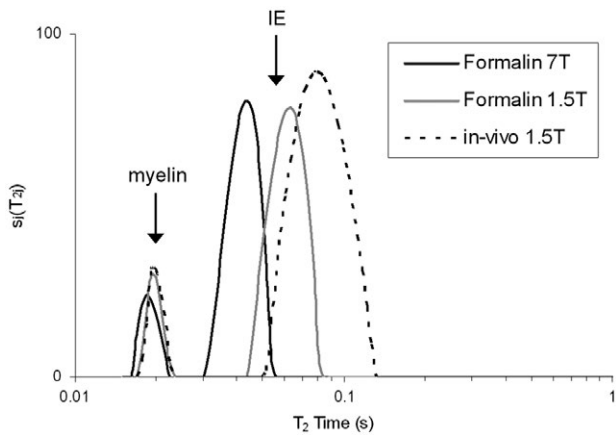


Figure 2. T₂ distribution from multiple sclerosis (MS) normal-appearing white matter (NAWM) in formalin at 7T (black), 1.5T (gray) and *in vivo* (light gray). All three distributions have a similar shape, showing two distinct peaks with the myelin water peak on the left and intra/extracellular (IE) component on the right. However, the IE component is shifted to shorter times for the 1.5T formalin sample, and even shorter for the 7T formalin sample when compared to *in vivo*. (Reprinted from *NeuroImage*. 2008;40(4): Laule C, Kozlowski P, Leung E, Li DKB, Mackay AL, Moore GRW. Myelin water imaging of multiple sclerosis at 7 T: Correlations with histopathology. pages 1575–1580, Figure 1, Copyright 2008, with permission from Elsevier).

with relative axonal sparing (**Figure 3**) (111). Visual correspondence between MRI and histology has improved significantly with the advent of higher field strength MR

systems that can produce MR images from much thinner volumes of tissue (Figure 4, 1mm thick at 7T (80) vs. Figure 3, 5mm thick at 1.5T). Further quantitative brain studies showed a tight relationship between the strength of the short-T₂ signal and the optical density of myelin staining as indicated by the myelin phospholipid stain Luxol Fast Blue (LFB) (63,96,141,146). (Figure 5) (75,76). Likewise, comparisons between MWF and myelin staining in human spinal cord also show excellent correspondence between the MR and histology markers for myelin (Figure 6) (88). As a consequence, the distribution of the short-T₂ component has been referred to as the “myelin water map.”

In addition to the above mentioned human validation studies, a number of animal studies have also demonstrated a strong correlation between myelin water and various myelin histological stains in both peripheral nervous system (121,132,158,168,185) and CNS animal models (45,67,68,100,161).

IN VIVO APPLICATIONS OF MYELIN WATER IMAGING IN RESEARCH AND CLINICAL TRIALS

Myelin variation in healthy brain and spinal cord white matter

Initial *in vivo* studies by MacKay *et al* of the brain almost 25 years ago demonstrated MWF of white matter to be substantially higher than gray matter, and regional

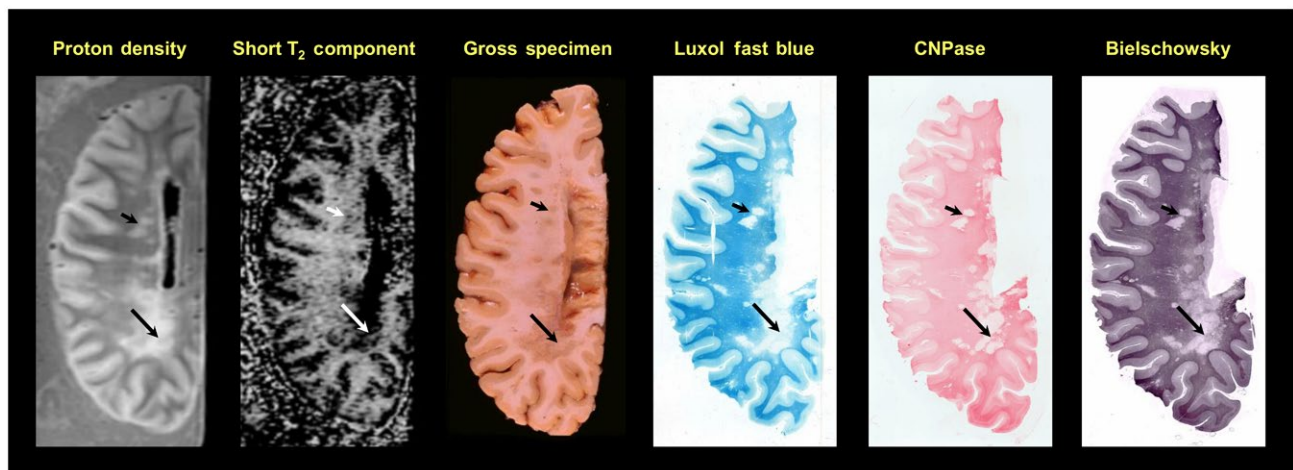


Figure 3. 58-year-old male with a 34-year history of secondary progressive multiple sclerosis (MS) with clinical evidence of optic, cerebellar and spinal involvement. Note the large, irregular lesion in the periventricular occipital white matter, which appears as an area of increased signal on the proton density scan, an area of absent signal on the myelin water/short-T₂ component distribution, and an area of gray discoloration of the white matter in the gross photograph. A band of reduced signal is seen in the lesion on both scans and correlates with the gross appearance (long arrows). More rostrally, several smaller lesions are evident (short arrows), which appear as areas of reduced intensity on the short-T₂ component image. The Luxol fast blue and 2',3'-cyclic nucleotide 3'-phosphohydrolase

(CNPase) stains show absence of myelin in most regions of the large periventricular occipital lesion. The Bielschowsky stain for axons is reduced in the lesions but not to the degree of the myelin stains. The faint band detected by the short-T₂ distribution component and the proton density scan is particularly evident on the CNPase stain (long arrows). (Moore, G.R.W., Leung, E., MacKay, A.L., Vavasour, I.M., Whittall, K.P., Cover, K.S., Li, D.K., Hashimoto, S.A., Oger, J., Sprinkle, T.J., Paty, D.W. A pathology-MRI study of the short-T₂ component in formalin-fixed multiple sclerosis brain. *Neurology* 2000;55(10):1506–1510. Figure 1. Published by The American Academy of Neurology, with permission. <http://n.neurology.org/content/55/10/1506.long>).

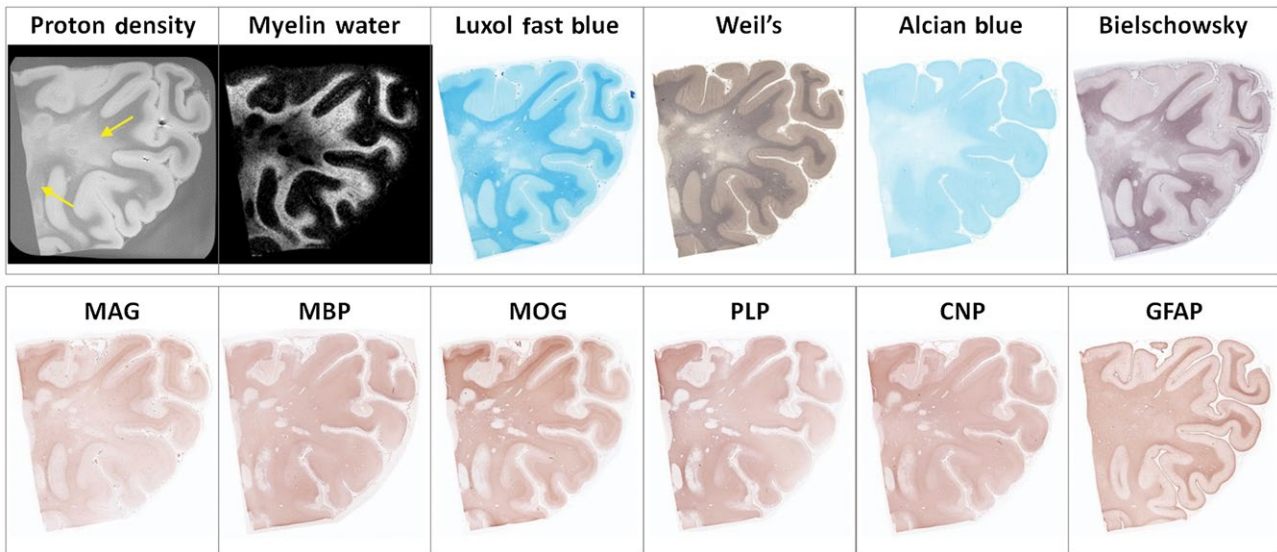


Figure 4. Example of diffusely abnormal white matter (DAWM) at 7T with corresponding myelin water map and histological stains for phospholipids (Luxol fast blue, Weil's), sialic acid groups (Alcian Blue), axons (Bielschowsky), myelin proteins (myelin-associated glycoprotein (MAG), myelin basic protein (MBP), myelin oligodendrocyte protein (MOG), proteolipid protein (PLP), 2',3'-cyclic nucleotide 3'-phosphohydrolase (CNP)), and astrocytes (GFAP). DAWM, characterized by an area of reduced intensity on the proton density (arrows) and myelin water map, matches a region of reduced staining intensity on the Luxol Fast Blue, Weil's, Alcian Blue, Bielschowsky,

and, to a lesser degree, MAG stains. Several small plaques are seen within this region. Note the improvement in resolution in this high-field strength compared to that at 1.5T shown in Figure 3. (Laule, C., Pavlova, V., Leung, E., Zhao, G., MacKay, A.L., Kozlowski, P., Traboulsee, A.L., Li, D.K., Moore, G.R.W. Diffusely abnormal white matter in multiple sclerosis: further histologic studies provide evidence for a primary lipid abnormality with neurodegeneration. *Journal of Neuropathology and Experimental Neurology* 2013; 72(1): 42–52, Figure 2, by permission of Oxford University Press and the American Association of Neuropathologists)

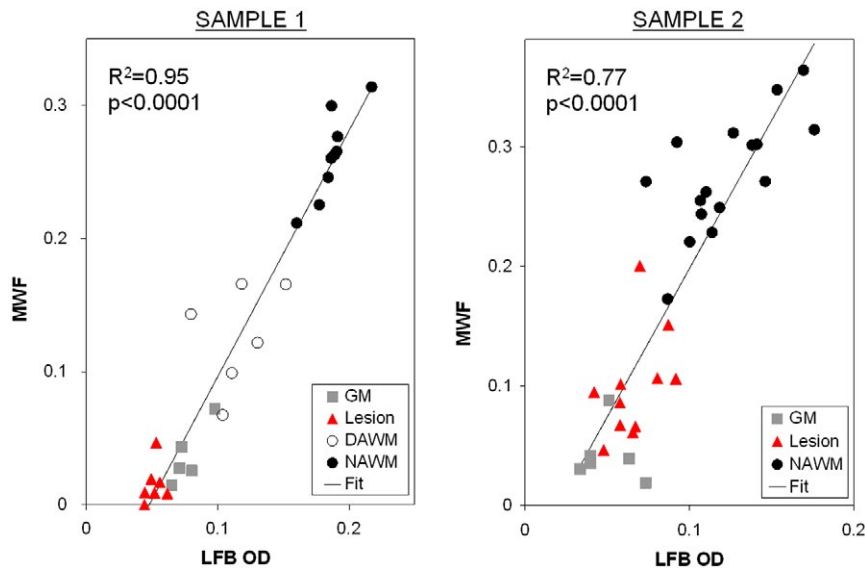


Figure 5. Examples of the quantitative correlation between myelin water fraction (MWF) and Luxol Fast Blue optical density (LFB OD) for gray matter (GM), lesion, diffusely-abnormal white matter (DAWM), and normal appearing white matter (NAWM) for 2 multiple sclerosis (MS)

cases. (Reprinted from *NeuroImage*. 2008;40(1): Laule C, Kozlowski P, Leung E, Li DKB, Mackay AL, Moore GRW. Myelin water imaging of multiple sclerosis at 7 T: Correlations with histopathology. pages 1575–1580, Figure 4, Copyright 2008, with permission from Elsevier).

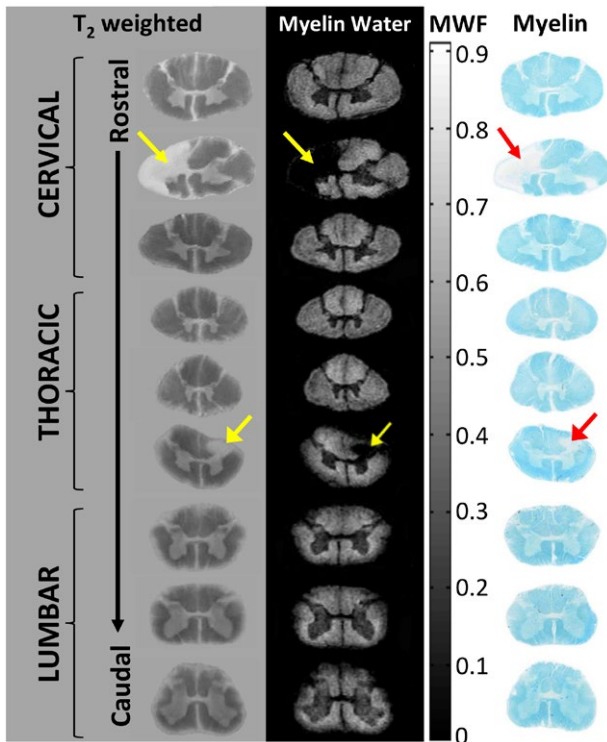


Figure 6. Magnetic resonance imaging (MRI) and corresponding histology from a formalin-fixed multiple sclerosis (MS) spinal cord. Cervical, thoracic, and lumbar regions show anatomical variation in myelin with white matter showing increased myelin water relative to the central gray matter butterfly. MS lesions (arrows) demonstrate myelin water loss. Staining for myelin (Luxol Fast Blue) demonstrates excellent correspondence between MRI and histology. (adapted from Figure 1a, Laule, C., Yung, A., Pavolva, V., Bohnet, B., Kozlowski, P., Hashimoto, S.A., Yip, S., Li, D.K., Moore, G.R.W. High-resolution myelin water imaging in post-mortem multiple sclerosis spinal cord: A case report. *Multiple Sclerosis* Oct 22 2016, 1485–1489, published by SAGE Publications).

variation of MWF across different white matter structures (97); this observation has been confirmed by numerous studies since (11,20,85,123,180,189). Frontal lobe MWF is correlated with age, as well as years of education and reading IQ in healthy adults (44,73). mcDESPOT-derived MWF shows a positive correlation between physical activity level and MWF in the right parahippocampal cingulum (16) and one study found regional differences in MWF of the corpus callosum between males and females (91). Reproducibility and reliability of MWF in healthy controls, both at a single site and multiple sites is very good (14,103,171,174).

Myelin water techniques applied in the brain can also be used to study spinal cord myelination. However, spinal cord myelin water imaging studies are far less common, since imaging the spinal cord is difficult for a number of reasons including the small diameter of the cord, cardiac and respiratory motion, magnetic field inhomogeneities, and the presence of flow from CSF. Nevertheless, it is feasible to measure MWF in the spinal cord *in vivo*. MWF is approximately 50% higher in spinal cord than normal brain white matter and varies along the length of the cord (66,87,98,105,193). Younger adults (20–30 years old) have a higher cervical cord MWF compared to older (50–75 year) study participants (98). An in-depth review of myelin water in the cord can be found elsewhere (78).

The aforementioned work, which characterizes MWF in controls and demonstrates sufficiently stable reproducibility, supports the application of myelin water imaging in disease states.

Multiple sclerosis plaques

Much of the pioneering *in vivo* work in myelin water imaging has been studies of MS. MS plaques, or lesions, show variably decreased MWF (Figure 7) (38,58,64,85,93,97,122,166,171,180), averaging approximately half that of

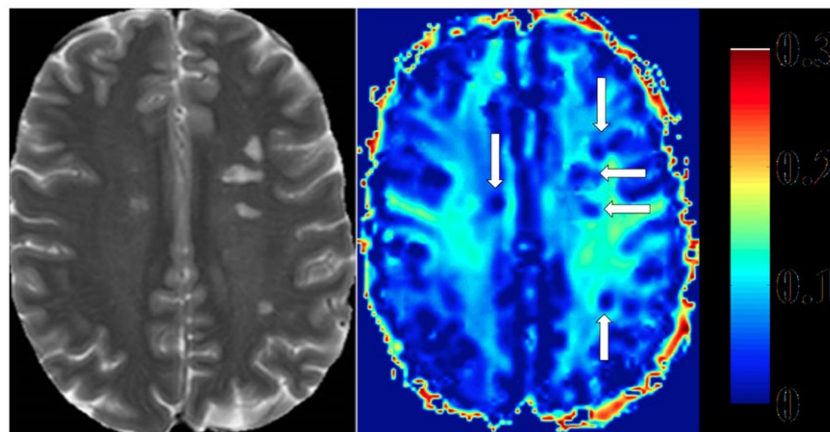


Figure 7. Heat map of myelin water fraction. Left side: T₂ weighted image of a Multiple Sclerosis (MS) patient. Right side: heat map of a myelin water image (MWF). T₂-hyperintense MS-lesions show clear reductions of myelin water fraction (MWF) (white arrows, right side). (Faizy TD, Thaler C, Kumar

D, Sedlacik J, Brooks G, Grosser M, Stellmann J-P, Heesen C, Fiehler J, Siemonsen S. (2016) Heterogeneity of Multiple Sclerosis Lesions in Multislice Myelin Water Imaging. *PLoS ONE* 11(6): e0151496. <https://doi.org/10.1371/journal.pone.0151496>, Figure 2).

normal-appearing white matter (NAWM) (85). This variability in MWF is probably reflective of the myelin content or pathology in different lesions. Indeed, MWF can vary between lesions change to observed on T_2 -weighted imaging, black holes evident on T_1 -weighted imaging and lesions with contrast enhancement (38,85,166). MWF can also be used to distinguish plaques based on their age, with older lesions change to showing a larger reduction in myelin water (178). The difference in MWF between new and old lesions suggests there is less advanced demyelination in new lesions or possibly ongoing remyelination which eventually fails in older lesions. Longitudinal study of MWF can provide insights into demyelination and remyelination in plaques, where a much as reduction in MWF in some lesions can be followed by MWF increase, suggesting remyelination over time (90,171,176).

Multiple sclerosis normal-appearing white matter

It has become increasingly apparent that what on routine MRI and casual histopathologic examination appears to be “normal-appearing white matter” is far from normal when more sophisticated tools in either of these spheres are used for interrogation of this region (110). Furthermore, these changes in MS NAWM are clinically relevant as they present very early in the course of the disease at the time of the first clinical presentation, and they correlate with disability, cognitive impairment, and the degree of brain atrophy (104).

The literature prior to the MRI era showed conflicting results with respect to MS NAWM neurochemistry and myelin damage (108). Some studies showed reductions in total phospholipid (23,49,136), phosphatidylserine (116), phosphatidylinositol (116), fatty acids particularly linoleic acid (9,49), cerebroside (1,135,136), sulfatide (5), the gangliosides GM4, GM1, GD1b, GQ1b (195). Other studies showed increased levels of cholesterol esters in NAWM (1,23,195). However, others reported normal levels of cholesterol esters (194), total cholesterol (194), total phospholipids (194), ethanolamine phospholipids (24), cerebroside (24), and sulfatide (24). In addition, while a variety of enzymes were found to be increased in NAWM, these results were also inconsistent (108). At the time, it was felt that these discrepant results were due the inadvertent inclusion of small macroscopically invisible plaques in the material assayed as NAWM and it was thought that biochemically NAWM was truly normal (163). Nevertheless, the very few neuropathologic studies of MS NAWM showed subtle abnormalities that could not be necessarily considered plaques. These included perivascular inflammation, perivascular lipofuscin deposition, cells with increased numbers of lysosomes, and occasional demyelination (3). Subsequent studies showed microglial activation (4), upregulation of factors involved in Class II Major Histocompatibility Complex (MHC) expression (50), expression of peripheral benzodiazepine binding sites (50), upregulation of osteopontin and α B-crystallin (150), extracellular matrix enzymes, and modification of extracellular matrix

components (154). Further studies showed blood–brain barrier breakdown in MS NAWM (61,128).

Very consistently, however, is the axonal loss that is evident in NAWM (36) and this loss correlates with plaque volume, consistent with the notion that it is due to Wallerian degeneration as a consequence of axons transected in plaques (37). Furthermore, this axonal loss appears to involve small-diameter axons predominately (28). Evidence for axonal degeneration is also apparent in the upregulation of ephrin A1 and receptors to ephrin-A3, -A4, and -A7 (153) and axonal amyloid precursor protein, dephosphorylated neurofilament, and neuropeptide Y receptor Y1 in periplaque white matter (33). An important driver of neurodegeneration in MS NAWM may be the bystander effect on the axon by the products of inflammatory infiltrates, which, while mild in degree, are scattered throughout the NAWM (71), and may be sequestered behind the blood–brain barrier (74).

There is compelling evidence from unconventional MRI techniques for abnormalities in NAWM. Reinforcing the neuropathologic findings of axonal degeneration and loss in NAWM is the finding of reduced NAA by MRS (27). In general, MRI-demonstrable axonal degeneration does not correlate with plaque load, suggesting that factors in addition to Wallerian degeneration may contribute to neurodegeneration in NAWM (104). Numerous studies support widespread and varying abnormalities in MS NAWM including increases in creatine (57), myo-inositol (42), choline (57), and lipid peaks (114), a higher apparent diffusion coefficient (187), reduced fractional anisotropy (51), reduced magnetization transfer ratio (43), prolonged T_1 (170), and increased total water content (85).

There is also strong *in vivo* MR evidence of myelin damage in MS NAWM. When compared to healthy controls, MWF is reduced in brain NAWM by 6%–37% (38,64,85,90,122) and in spinal cord by 11%–25% (87,193). NAWM MWF can differentiate between different subtypes of MS, with greater myelin loss found in more progressive forms of the disease (62), and reduction of MWF is related to increased clinical disability (62,64). Changes in NAWM MWF can also be discerned over time (60); for example, in untreated relapsing-remitting MS patients there was an 8% reduction in brain MWF over 5 years (175), suggesting that chronic, progressive myelin damage is an evolving process occurring over many years. Longitudinal assessment of brain myelin water in non-lesional tissue has also been successfully used in clinical trials, with a recent study demonstrating NAWM MWF stability after 24 months on MS disease-modifying therapy (179). Changes in NAWM MWF can also be reliably detected in the spinal cord, with one study showing a 10% myelin loss in primary progressive MS cervical cord over 2 years, while controls remained stable, suggesting ongoing demyelination may be contributing to the disease process in this subgroup of patients (87).

The histopathologic correlate of the NAWM MWF abnormality has not yet been determined. Based on the discussion of the origin of the MWF above, it could represent a change in the periodicity of the spacing of myelin

lamellae in the myelin which by the usual histologic stains appears normal. Another alternative is that it may simply be a reflection of the concomitant widespread loss of axons in NAWM (36,37,149). Supporting these notions, one study showed that NAWM, as defined by magnetization transfer imaging, showed histopathologic correlates that were spatially dependent (106). NAWM near a plaque shows correlation with microglial and axonal pathology, that latter presumably being secondary to axonal damage within the plaque. Whereas, NAWM remote from the plaque correlates with microglial activation but not axonal damage, suggesting again a factor in addition to Wallerian degeneration is operative in these regions (27,106).

Multiple sclerosis diffusely-abnormal white matter

In 2000, Zhao, Li, and colleagues first described “dirty-appearing white matter” in routine MRI in MS (197). This abnormality, which has subsequently been referred to as “diffusely-abnormal white matter” (DAWM), has a signal intensity intermediate between that of NAWM and that of plaque, similar to gray matter on proton density and T_2 weighted imaging. It is evident in approximately 20%–25% of MS patients, who tend to have a more rapidly progressive clinical course (196). DAWM shows ill-defined boundaries and is sometimes adjacent to a plaque, particularly in the periventricular occipital white matter.

Pathologic studies have shown reduced myelin on the LFB stain and reduced numbers of axons in DAWM (145). There is also evidence of blood–brain barrier breakdown in DAWM (182). When the DAWM myelin abnormality is interrogated with a variety of stains, it is apparent that while LFB (96,141,146) and another phospholipid stain, the Weil’s stain (186), are reduced in DAWM, immunohistochemical staining for various myelin proteins is relatively preserved (Figure 4), suggesting that there is a selective lipid abnormality in DAWM myelin (80,83,107). There is also a reduction of staining for sialic acid groups (on the Alcian blue stain) (80). Since the major source of sialic acid groups in the CNS is gangliosides, this finding suggests that in DAWM there is a perturbation of gangliosides, which are located particularly in the axolemma rather than the myelin sheath (Figure 1). Interestingly, the only myelin protein that is occasionally reduced in DAWM is myelin-associated glycoprotein (MAG) (80), which is located adjacent to the adaxonal space and serves as the ligand that binds the myelin sheath to the axon by interaction with its axolemmal ganglioside receptors GD1a and GT1b (48,101). Axonal loss, as evident on the modified Bielschowsky stain, is often but not always evident in DAWM, indicating neurodegeneration may occur in DAWM and this might possibly be a result of the MAG-axolemmal ganglioside perturbation.

It is also of considerable interest, from the point of view of myelin biology and imaging, that the MWF is exquisitely sensitive for the detection of DAWM, showing 23% reduction of MWF in this region *in vivo* (83) and 30% loss post-mortem (80). Again, given that it is thought

the MWF emanates from restricted water in the tight lamellar compaction of myelin, we postulate that the lipid abnormality in DAWM leads to myelin membrane permeability to water, which would result in widening of the myelin lamellar water reservoir resulting in reduction of the value of the short- T_2 component and also lead to the observed increase in mean T_2 and total water content seen *in vivo* (83). This, however, would not necessarily affect the concentration of myelin protein constituents within the myelin lipid bilayers, with the exception of the perturbed ganglioside-MAG interactions and subsequent axonal degeneration in more advanced DAWM pathology. Other quantitative MRI studies also show abnormalities in DAWM (46,79,83,126,139) and differences in DAWM in different clinical subtypes of MS, with primary progressive MS showing higher T_1 and lower magnetization transfer ratio than the secondary progressive form of the disease (183). Clearly, further research is necessary to sort out the complex but fascinating changes in DAWM, which may well be important clinically and could represent the early events in propagating the expansion of the MS plaque that it borders.

Neurological applications beyond MS

Beyond MS, myelin water imaging has been used to study many other neurological disease applications include neuromyelitis optica (58,99), schizophrenia and first episode psychosis (44,73), phenylketonuria (151), autism (30), stroke (14), neurofibromatosis (10), Niemann–Pick disease (25), primary lateral sclerosis (65), amyotrophic lateral sclerosis (65), concussion (192), and Krabbe disease (86). Other spinal cord applications are also feasible, for example, a recent study of cervical spondylotic myelopathy demonstrated a correlation between MWF in the dorsal columns and functional measures of myelin through somatosensory evoked potential latency times (92).

OTHER MR METHODS SENSITIVE TO MYELIN

Several other MRI techniques have been proposed to be sensitive to changes in myelin. **Magnetization transfer (MT)** imaging measures decreases in MR signal following off-resonance excitations (191); the effect is typically quantified by a magnetization transfer ratio, which is sensitive to small differences between groups. There is an extensive literature on using MT to study myelination in MS (7) and several studies have showed correlation between MT parameters and histological measures of myelin (19,144). A limitation of using MT to monitor myelin is that while a change in myelin will cause a change in MT, a change in MT is not necessarily due to a change in myelin. Changes in other tissue components such as axons and glia, as well as changes in water content due to inflammation or edema will result in changes in MT (112,177). A newer magnetization transfer related method termed **inhomogeneous magnetization transfer (ihMT)** shows promise for being

more specific to CNS lipids; given that myelin is 70%–80% lipids and ihMT correlates well with MWF, this is an exciting area of ongoing myelin imaging research (34,172,173). Several metrics acquired using **diffusion tensor imaging (DTI)**, which examines water movement, have been linked to myelin. Most notably the perpendicular component of the diffusion tensor (often called lambda perp or radial diffusivity) is inversely related to myelination in animal models (155,184). However, the presence of edema and neuroanatomy such as crossing fibers can confound DTI measurements. More sophisticated diffusion modeling and analysis approaches are now emerging including constrained spherical deconvolution (CSD), Q-ball imaging (QBI), diffusion orientation transform (DOT), persistent angular structure (PAS), and neurite orientation dispersion and density imaging (NODDI) and diffusion basis spectrum imaging (DBSI) which may provide more specific links to tissue components, including myelin (143,184). Finally, **ultrashort echo time (UTE)** measures signal from non-water sources of hydrogen, including, but not limited to, the lipids and proteins that make up myelin (137). Several studies have used UTE for myelin measurement (15,55,190) and, as this method is becoming more commonly available on newer MR systems, it is expected that research on using UTE for myelin imaging will continue to expand (31,39,148).

CONCLUSION

There have been numerous substantial advances in myelin imaging and exciting research is ongoing in this area. New techniques or modifications of currently employed techniques to demonstrate myelin *in vivo* will continue to be developed. All of these new methodologies, however, must pass the scrutiny of histopathologic validation before they can be accepted as appropriate tools to image myelin and its disorders.

ACKNOWLEDGMENTS

We would like to thank the patients and their families who have contributed so generously to our research studies. Grant funding support is provided by the Multiple Sclerosis Society of Canada (CL, GRWM), Natural Sciences and Engineering Research Council of Canada (NSERC) (CL), and the International Collaboration on Repair Discoveries (ICORD) (CL, GRWM). The authors would also like to acknowledge the collaborations of our colleagues at the University of British Columbia (UBC) MRI Research Centre, the UBC MS/MRI Research Group, and the UBC Hospital MS Clinic.

CONFLICT OF INTEREST

CL has nothing to declare. GRWM has received a grant-in-aid of research from Berlex Canada, has acted as a consultant for Schering, and has received honoraria from

Teva for teaching. He is a member of the Medical Advisory Committee of the Multiple Sclerosis Society of Canada.

REFERENCES

- Adams CW, Hallpike JF, Bayliss OB (1971) Histochemistry of myelin. 13. Digestion of basic protein outside acute plaques of multiple sclerosis. *J Neurochem* **18**:1479–1483.
- Akhondi-Asl A, Afacan O, Mulkern RV, Warfield SK (2014) T(2)-relaxometry for myelin water fraction extraction using wald distribution and extended phase graph. *Med Image Comput Comput-Assisted Intervention: MICCAI Int Conf Med Image Comput Comput-Assisted Intervention* **17**(Pt 3):145–152.
- Allen IV (1984) Demyelinating diseases. In: Greenfield's Neuropathology. J Adams, J Corsellis, L DuChen(eds), pp. 338–384. John Wiley and Sons: New York.
- Allen IV, McQuaid S, Mirakhor M, Nevin G (2001) Pathological abnormalities in the normal-appearing white matter in multiple sclerosis. *Neurol Sci* **22**:141–144.
- Alling C, Vanier MT, Svennerholm L (1971) Lipid alterations in apparently normal white matter in multiple sclerosis. *Brain Res* **35**:325–336.
- Alonso-Ortiz E, Levesque IR, Pike GB (2014) MRI-based myelin water imaging: a technical review. *Magn Reson Med* **73**:70–81
- Arnold DL, Dalton CM, Schmierer K, Pike GB, Miller DH (2013) Imaging of demyelination and remyelination in multiple sclerosis. In: *Myelin Repair and Neuroprotection in Multiple Sclerosis*. ID Duncan, RJ Franklin (eds.), pp. 233–253. Springer: Boston, MA.
- Arnold DL, Matthews PM, Francis GS, O'Connor J, Antel JP (1992) Proton magnetic resonance spectroscopic imaging for metabolic characterization of demyelinating plaques. *Ann Neurol* **31**:235–241.
- Baker RW, Thompson RH, Zilkha KJ (1963) Fatty-acid composition of brain lecithins in multiple sclerosis. *Lancet* **1**:26–27.
- Billiet T, Madler B, D'Arco F, Peeters R, Deprez S, Plasschaert E, Leemans A, Zhang H, den Bergh BV, Vandenbulcke M, Legius E, Sunaert S, Emsell L (2014) Characterizing the microstructural basis of “unidentified bright objects” in neurofibromatosis type 1: a combined *in vivo* multicomponent T₂ relaxation and multi-shell diffusion MRI analysis. *Neuroimage Clin* **4**:649–658.
- Billiet T, Vandenbulcke M, Madler B, Peeters R, Dhollander T, Zhang H, Deprez S, Van den Bergh BR, Sunaert S, Emsell L (2015) Age-related microstructural differences quantified using myelin water imaging and advanced diffusion MRI. *Neurobiol Aging* **36**:2107–2121.
- Bjartmar C, Battistuta J, Terada N, Dupree E, Trapp BD (2002) N-acetylaspartate is an axon-specific marker of mature white matter *in vivo*: a biochemical and immunohistochemical study on the rat optic nerve. *Ann Neurol* **51**:51–58.
- Bo L, Vedeler CA, Nyland HI, Trapp BD, Mork SJ (2003) Subpial demyelination in the cerebral cortex of multiple sclerosis patients. *J Neuropathol Exp Neurol* **62**:723–732.
- Borich MR, Mackay AL, Vavasour IM, Rauscher A, Boyd LA (2013) Evaluation of white matter myelin water fraction in chronic stroke. *Neuroimage Clin* **2**:569–580.
- Boucneau T, Cao P, Tang S, Han M, Xu D, Henry RG, Larson PEZ (2018) *In vivo* characterization of brain ultrashort-T₂ components. *Magn Reson Med* **80**:726–735.

16. Bracht T, Jones DK, Bells S, Walther S, Drakesmith M, Linden D (2016) Myelination of the right parahippocampal cingulum is associated with physical activity in young healthy adults. *Brain Struct Funct* **221**:4537–4548.
17. Carswell R (1838) *Pathological anatomy*. Orme, Brown, Green and Longman: London.
18. Charcot JM (1868) Histologie de la sclérose en plaques. *Gaz Hopit Civils Milit* **41**:554,7,66.
19. Chen JT, Collins DL, Freedman MS, Atkins HL, Arnold DL, The Canadian MSBMTSG (2005) Local magnetization transfer ratio signal inhomogeneity is related to subsequent change in MTR in lesions and normal-appearing white-matter of multiple sclerosis patients. *Neuroimage* **25**:1272–1278.
20. Chia CLL, Bjarnason TA, Mackay AL, Pike GB (2006) Cross-site reproducibility of myelin water estimates. In: 14th Annual Meeting of the International Society of Magnetic Resonance in Medicine, p. 2520: Seattle, USA.
21. Compston A (1988) The 150th anniversary of the first depiction of the lesions of multiple sclerosis. *J Neurol Neurosurg Psychiatry* **51**:1249–1252
22. Cruveilhier J (1842) *Anatomie pathologique du corps humain; descriptions, avec figures lithographiées et coloriées; des diverses altérations morbides dont le corps humain est susceptible*. Vol 2. Paris: J.B. Baillière, 40 livraisons, 1829–42.
23. Cumings JN (1955) Lipid chemistry of the brain in demyelinating diseases. *Brain* **78**:554–563.
24. Cuzner ML, Davison AN (1973) Changes in cerebral lysosomal enzyme activity and lipids in multiple sclerosis. *J Neurol Sci* **19**:29–36.
25. Davies-Thompson J, Vavasour I, Scheel M, Rauscher A, Barton JJ (2016) Reduced myelin water in the white matter tracts of patients with Niemann-pick disease type C. *AJNR Am J Neuroradiol* **37**:1487–1489.
26. Dawson J (1916) The histology of disseminated sclerosis. *Trans R Soc Edin Reproduced by the Montreal Neurological Institute, Montreal* **50**:517–540.
27. De Stefano N, Narayanan S, Francis SJ, Smith S, Mortilla M, Tartaglia MC, Bartolozzi ML, Guidi L, Federico A, Arnold DL (1965) Diffuse axonal and tissue injury in patients with multiple sclerosis with low cerebral lesion load and no disability. *Arch Neurol*. **59**:1565–1571.
28. DeLuca GC, Ebers GC, Esiri MM (2004) Axonal loss in multiple sclerosis: a pathological survey of the corticospinal and sensory tracts. *Brain* **127**(Pt 5):1009–1018.
29. Deoni SC, Rutt BK, Arun T, Pierpaoli C, Jones DK (2008) Gleaning multicomponent T₁ and T₂ information from steady-state imaging data. *Magn Reson Med* **60**:1372–1387.
30. Deoni SC, Zinkstok JR, Daly E, Ecker C, Williams SC, Murphy DG (2015) White-matter relaxation time and myelin water fraction differences in young adults with autism. *Psychol Med* **45**:795–805.
31. Du J, Ma G, Li S, Carl M, Szeverenyi NM, VandenBerg S, Corey-Bloom J, Bydder GM (2014) Ultrashort echo time (UTE) magnetic resonance imaging of the short T₂ components in white matter of the brain using a clinical 3T scanner. *Neuroimage* **87**:32–41.
32. Du YP, Chu R, Hwang D, Brown MS, Kleinschmidt-DeMasters BK, Singel D, Simon JH (2007) Fast multislice mapping of the myelin water fraction using multicompartiment analysis of T₂* decay at 3T: a preliminary postmortem study. *Magn Reson Med* **58**:865–870.
33. Dziedzic T, Metz I, Dallenga T, Konig FB, Muller S, Stadelmann C, Bruck W (2010) Wallerian degeneration: a major component of early axonal pathology in multiple sclerosis. *Brain Pathol* **20**:976–985.
34. Ercan E, Varma G, Madler B, Dimitrov IE, Pinho MC, Xi Y, Wagner BC, Davenport EM, Maldjian JA, Alsop DC, Lenkinski RE, Vinogradov E (2018) Microstructural correlates of 3D steady-state inhomogeneous magnetization transfer (ihMT) in the human brain white matter assessed by myelin water imaging and diffusion tensor imaging. *Magn Reson Med*. [Epub ahead of print].
35. Estes ML, Rudick RA, Barnett GH, Ransohoff RM (1990) Stereotactic biopsy of an active multiple sclerosis lesion. Immunocytochemical analysis and neuropathologic correlation with magnetic resonance imaging. *Arch Neurol* **47**:1299–1303.
36. Evangelou N, Esiri MM, Smith S, Palace J, Matthews PM (2000) Quantitative pathological evidence for axonal loss in normal appearing white matter in multiple sclerosis. *Ann Neurol* **47**:391–395.
37. Evangelou N, Konz D, Esiri MM, Smith S, Palace J, Matthews PM (2000) Regional axonal loss in the corpus callosum correlates with cerebral white matter lesion volume and distribution in multiple sclerosis. *Brain* **123**(Pt 9):1845–1849.
38. Faizy TD, Thaler C, Kumar D, Sedlacik J, Broocks G, Grosser M, Stellmann JP, Heesen C, Fiehler J, Siemonsen S (2016) Heterogeneity of multiple sclerosis lesions in multislice myelin water imaging. *PLoS ONE*. **11**:e0151496.
39. Fan SJ, Ma Y, Zhu Y, Searleman A, Szeverenyi NM, Bydder GM, Du J (2018) Yet more evidence that myelin protons can be directly imaged with UTE sequences on a clinical 3T scanner: bicomponent T₂* analysis of native and deuterated ovine brain specimens. *Magn Reson Med* **80**:538–547.
40. Fatouros PP, Marmarou A (1999) Use of magnetic resonance imaging for *in vivo* measurements of water content in human brain: method and normal values. *J Neurosurg* **90**:109–115.
41. Ferguson B, Matyszak MK, Esiri MM, Perry VH (1997) Axonal damage in acute multiple sclerosis lesions. *Brain* **120**(Pt 3):393–399.
42. Fernando KT, McLean MA, Chard DT, MacManus DG, Dalton CM, Miszkil KA, Gordon RM, Plant GT, Thompson AJ, Miller DH (2004) Elevated white matter myo-inositol in clinically isolated syndromes suggestive of multiple sclerosis. *Brain* **127**(Pt 6):1361–1369.
43. Filippi M, Campi A, Dousset V, Baratti C, Martinelli V, Canal N, Scotti G, Comi G (1995) A magnetization transfer imaging study of normal-appearing white matter in multiple sclerosis. *Neurology* **45**(3 Pt 1):478–482.
44. Flynn SW, Lang DJ, Mackay AL, Goghari V, Vavasour IM, Whittall KP, Smith GN, Arango V, Mann JJ, Dwork AJ, Falkai P, Honer WG (2003) Abnormalities of myelination in schizophrenia detected *in vivo* with MRI, and post-mortem with analysis of oligodendrocyte proteins. *Mol Psychiatry* **8**:811–820.
45. Gareau PJ, Rutt BK, Bowen CV, Karlik SJ, Mitchell JR (1999) *In vivo* measurements of multi-component T₂ relaxation behaviour in guinea pig brain. *Magn Reson Imaging* **17**:1319–1325.

46. Ge Y, Grossman RI, Babb JS, He J, Mannon LJ (2003) Dirty-appearing white matter in multiple sclerosis: volumetric MR imaging and magnetization transfer ratio histogram analysis. *AJNR Am J Neuroradiol* **24**: 1935–1940.
47. Gelman N, Ewing JR, Gorell JM, Spickler EM, Solomon EG (2001) Interregional variation of longitudinal relaxation rates in human brain at 3.0 T: relation to estimated iron and water contents. *Magn Reson Med* **45**:71–79.
48. Georgiou J, Tropak M, Roder J (2004) Myelin-associated glycoprotein gene. In: *Myelin Biology and Disorders*, Lazzarini R, Griffin J, Lassmann H, Nave K-A, Miller R, Trapp B (eds.), pp. 421–467. Elsevier Academic Press: San Diego, CA, USA.
49. Gerstl B, Kahnke MJ, Smith JK, Tavaststjerna MG, Hayman RB (1961) Brain lipids in multiple sclerosis and other diseases. *Brain* **84**:310–319.
50. Gobin SJ, Montagne L, Van Zutphen M, Van Der Valk P, Van Den Elsen PJ, De Groot CJ (2001) Upregulation of transcription factors controlling MHC expression in multiple sclerosis lesions. *Glia* **36**:68–77.
51. Guo AC, Jewells VL, Provenzale JM (2001) Analysis of normal-appearing white matter in multiple sclerosis: comparison of diffusion tensor MR imaging and magnetization transfer imaging. *AJNR Am J Neuroradiol* **22**:1893–1900.
52. Guo J, Ji Q, Reddick WE (2013) Multi-slice myelin water imaging for practical clinical applications at 3.0 T. *Magn Reson Med* **70**:813–822.
53. Haider L, Simeonidou C, Steinberger G, Hametner S, Grigoriadis N, Deretzi G, Kovacs GG, Kutzelnigg A, Lassmann H, Frischer JM (2014) Multiple sclerosis deep grey matter: the relation between demyelination, neurodegeneration, inflammation and iron. *J Neurol Neurosurg Psychiatry* **85**:1386–1395.
54. Höftberger R, Lassmann H (2017) Inflammatory demyelinating diseases of the central nervous system. *Handb Clin Neurol Vol 145, Neuropathology*. Kovacs GG, Alafuzoff I (eds). Amsterdam: Elsevier, pp 263–283.
55. Horch RA, Gore JC, Does MD (2011) Origins of the ultrashort-T₂ 1H NMR signals in myelinated nerve: a direct measure of myelin content? *Magn Reson Med* **66**:24–31.
56. Huitinga I, De Groot CJ, Van der Valk P, Kamphorst W, Tilders FJ, Swaab DF (2001) Hypothalamic lesions in multiple sclerosis. *J Neuropathol Exp Neurol* **60**:1208–1218.
57. Inglese M, Li BS, Rusinek H, Babb JS, Grossman RI, Gonen O (2003) Diffusely elevated cerebral choline and creatine in relapsing-remitting multiple sclerosis. *Magn Reson Med* **50**:190–195.
58. Jeong IH, Choi JY, Kim SH, Hyun JW, Joung A, Lee J, Kim HJ (2016) Comparison of myelin water fraction values in periventricular white matter lesions between multiple sclerosis and neuromyelitis optica spectrum disorder. *Mult Scler* **22**:1616–1620.
59. Kidd D, Barkhof F, McConnell R, Algra PR, Allen IV, Revesz T (1999) Cortical lesions in multiple sclerosis. *Brain* **122**(Pt 1):17–26.
60. King EM, Sabatier MJ, Hoque M, Kesar TM, Backus D, Borich MR (2018) Myelin status is associated with change in functional mobility following slope walking in people with multiple sclerosis. *Mult Scler J Exp Transl Clin* **4**:2055217318773540.
61. Kirk J, Plumb J, Mirakhur M, McQuaid S (2003) Tight junctional abnormality in multiple sclerosis white matter affects all calibres of vessel and is associated with blood-brain barrier leakage and active demyelination. *J Pathol* **201**:319–327.
62. Kitzler HH, Su J, Zeineh M, Harper-Little C, Leung A, Kremenchutzky M, Deoni SC, Rutt BK (2012) Deficient MWF mapping in multiple sclerosis using 3D whole-brain multi-component relaxation MRI. *Neuroimage* **59**:2670–2677.
63. Klüver H, Barrera E (1953) A method for the combined staining of cells and fibres in the nervous system. *J Neuropathol Exp Neurol* **12**:400–403.
64. Kolind S, Matthews L, Johansen-Berg H, Leite MI, Williams SC, Deoni S, Palace J (2012) Myelin water imaging reflects clinical variability in multiple sclerosis. *Neuroimage* **60**:263–270.
65. Kolind S, Sharma R, Knight S, Johansen-Berg H, Talbot K, Turner MR (2013) Myelin imaging in amyotrophic and primary lateral sclerosis. *Amyotrophic Lateral Scler Frontotemporal Degener* **14**:562–573.
66. Kolind SH, Deoni SC (2011) Rapid three-dimensional multicomponent relaxation imaging of the cervical spinal cord. *Magn Reson Med* **65**:551–556.
67. Kozłowski P, Liu J, Yung AC, Tetzlaff W (2008) High-resolution myelin water measurements in rat spinal cord. *Magn Reson Med* **59**:796–802.
68. Kozłowski P, Rosicka P, Liu J, Yung AC, Tetzlaff W (2014) *In vivo* longitudinal myelin water imaging in rat spinal cord following dorsal column transection injury. *Magn Reson Imaging* **32**:250–258.
69. Kumar D, Hariharan H, Faizy TD, Borchert P, Siemonsen S, Fiehler J, Reddy R, Sedlacik J (2018) Using 3D spatial correlations to improve the noise robustness of multi component analysis of 3D multi echo quantitative T₂ relaxometry data. *Neuroimage* **178**:583–601.
70. Kumar D, Nguyen TD, Gauthier SA, Raj A (2012) Bayesian algorithm using spatial priors for multiexponential T(2) relaxometry from multiecho spin echo MRI. *Magn Reson Med* **68**:1536–1543.
71. Kutzelnigg A, Lucchinetti CF, Stadelmann C, Bruck W, Rauschka H, Bergmann M, Schmidbauer M, Parisi JE, Lassmann H (2005) Cortical demyelination and diffuse white matter injury in multiple sclerosis. *Brain* **128**(Pt 11):2705–2712.
72. Labadie C, Lee JH, Rooney WD, Jarchow S, Aubert-Frecon M, Springer CS Jr, Moller HE (2014) Myelin water mapping by spatially regularized longitudinal relaxographic imaging at high magnetic fields. *Magn Reson Med* **71**:375–387.
73. Lang DJ, Yip E, MacKay AL, Thornton AE, Vila-Rodriguez F, MacEwan GW, Kopala LC, Smith GN, Laule C, MacRae CB, Honer WG (2014) 48 echo T(2) myelin imaging of white matter in first-episode schizophrenia: evidence for aberrant myelination. *Neuroimage Clin* **6**:408–414.
74. Lassmann H, van Horssen J, Mahad D (2012) Progressive multiple sclerosis: pathology and pathogenesis. *Nat Rev Neurol* **8**:647–656.
75. Laule C, Kozłowski P, Leung E, Li DK, Mackay AL, Moore GR (2008) Myelin water imaging of multiple sclerosis at 7 T: correlations with histopathology. *Neuroimage* **40**:1575–1580.
76. Laule C, Leung E, Li DK, Traboulsee AL, Paty DW, MacKay AL, Moore GR (2006) Myelin water imaging in multiple sclerosis: quantitative correlations with histopathology. *Mult Scler* **12**:747–753.

77. Laule C, Leung E, Lis DK, Traboulsee AL, Paty DW, MacKay AL, Moore GR (2006) Myelin water imaging in multiple sclerosis: quantitative correlations with histopathology. *Mult Scler* **12**:747–753.
78. Laule C, MacKay AL (2014) T₂ Relaxation. In: Quantitative MRI of the Spinal Cord, Cohen-Adad J, Wheeler-Kingshott CA (eds.), pp. 179–204. Elsevier: Academic Press/Elsevier: Cambridge, MA.
79. Laule C, Moore GR, Leung E, Michelin E, MacKay AL, Vavasour IM, Oger J, Paty DW, Li DKB (2001) A serial study of dirty white matter in MS. *Mult Scler. (Suppl 1)*:S90.
80. Laule C, Pavlova V, Leung E, Zhao G, MacKay AL, Kozlowski P, Traboulsee AL, Li DK, Moore GR (2013) Diffusely abnormal white matter in multiple sclerosis: further histologic studies provide evidence for a primary lipid abnormality with neurodegeneration. *J Neuropathol Exp Neurol* **72**:42–52.
81. Laule C, Vavasour IM, Kolind SH, Li DK, Traboulsee TL, Moore GR, Mackay AL (2007) Magnetic resonance imaging of myelin. *Neurotherapeutics* **4**:460–484.
82. Laule C, Vavasour IM, Kolind SH, Traboulsee AL, Moore GRW, Li DKB, MacKay AL (2007) Long T₂ water in multiple sclerosis: what else can we learn from multi-echo T₂ relaxation? *J Neurol* **254**:1579–1587.
83. Laule C, Vavasour IM, Leung E, Li DK, Kozlowski P, Traboulsee AL, Oger J, Mackay AL, Moore GR (2011) Pathological basis of diffusely abnormal white matter: insights from magnetic resonance imaging and histology. *Mult Scler* **17**:144–150.
84. Laule C, Vavasour IM, Madler B, Kolind SH, Sirrs SM, Brief EE, Traboulsee AL, Moore GR, Li DK, Mackay AL (2007) MR evidence of long T(2) water in pathological white matter. *J Magn Reson Imaging* **26**:1117–1121.
85. Laule C, Vavasour IM, Moore GRW, Oger J, Li DKB, Paty DW, MacKay AL (2004) Water content and myelin water fraction in multiple sclerosis: A T₂ relaxation study. *J Neurol* **251**:284–293.
86. Laule C, Vavasour IM, Shahinfard E, Madler B, Zhang J, Li DKB, MacKay AL, Sirrs SM (2018) Hematopoietic stem cell transplantation in late-onset krabbe disease: no evidence of worsening demyelination and axonal loss 4 years post-allograft. *J Neuroimaging* **28**:252–255.
87. Laule C, Vavasour IM, Zhao Y, Traboulsee AL, Oger J, Vavasour JD, Mackay AL, Li DK (2010) Two-year study of cervical cord volume and myelin water in primary progressive multiple sclerosis. *Mult Scler* **16**:670–677.
88. Laule C, Yung A, Pavlova V, Bohnet B, Kozlowski P, Hashimoto SA, Yip S, Li DK, Moore GW (2016) High-resolution myelin water imaging in post-mortem multiple sclerosis spinal cord: a case report. *Mult Scler. Oct* **22**:1485–1489.
89. Lenz C, Klarhofer M, Scheffler K (2011) Feasibility of *in vivo* myelin water imaging using 3D multigradient-echo pulse sequences. *Magn Reson Med* **68**:523–528.
90. Levesque IR, Giacomini PS, Narayanan S, Ribeiro LT, Sled JG, Arnold DL, Pike GB (2010) Quantitative magnetization transfer and myelin water imaging of the evolution of acute multiple sclerosis lesions. *Magn Reson Med* **63**:633–640.
91. Liu F, Vidarsson L, Winter JD, Tran H, Kassner A (2010) Sex differences in the human corpus callosum microstructure: a combined T₂ myelin-water and diffusion tensor magnetic resonance imaging study. *Brain Res* **1343**:37–45.
92. Liu H, MacMillan EL, Jutzeler CR, Ljungberg E, MacKay AL, Kolind SH, Madler B, Li DKB, Dvorak MF, Curt A, Laule C, Kramer JLK (2017) Assessing structure and function of myelin in cervical spondylotic myelopathy: evidence of demyelination. *Neurology* **89**:602–610.
93. Llufriu S, Kornak J, Ratiney H, Oh J, Brennen D, Cree BA, Sampat M, Hauser SL, Nelson SJ, Pelletier D (2014) Magnetic resonance spectroscopy markers of disease progression in multiple sclerosis. *JAMA Neurol* **71**:840–847.
94. Louapre C, Bodini B, Lubetzki C, Freeman L, Stankoff B (2017) Imaging markers of multiple sclerosis prognosis. *Curr Opin Neurol* **30**:231–236.
95. Ludwin SK, Raine CS (2008) The neuropathology of multiple sclerosis. In: Multiple Sclerosis—A Comprehensive Text, Raine CS, McFarland H, Hohlfeld R (eds.), pp. 151–177, Elsevier Health Sciences: London, UK.
96. Lycette R, Danforth J, Koppel J, Olwin J (1970) The binding of iusol fast blur ARN by various biological lipids. *Staining Technol* **45**:155–160.
97. MacKay A, Whittall K, Adler J, Li D, Paty D, Graeb D (1994) *In vivo* visualization of myelin water in brain by magnetic resonance. *Magn Reson Med* **31**:673–677.
98. MacMillan EL, Madler B, Fichtner N, Dvorak MF, Li DK, Curt A, MacKay AL (2011) Myelin water and T(2) relaxation measurements in the healthy cervical spinal cord at 3.0T: repeatability and changes with age. *Neuroimage* **54**:1083–1090.
99. Manogaran P, Vavasour I, Borich M, Kolind SH, Lange AP, Rauscher A, Boyd L, Li DK, Traboulsee A (2016) Corticospinal tract integrity measured using transcranial magnetic stimulation and magnetic resonance imaging in neuromyelitis optica and multiple sclerosis. *Mult Scler* **22**:43–50.
100. McCreary CR, Bjarnason TA, Skihar V, Mitchell JR, Yong VW, Dunn JF (2009) Multiexponential T₂ and magnetization transfer MRI of demyelination and remyelination in murine spinal cord. *Neuroimage* **45**:1173–1182.
101. McKerracher L (2002) Ganglioside rafts as MAG receptors that mediate blockade of axon growth. *Proc Natl Acad Sci USA* **99**:7811–7813.
102. Menon RS, Allen PS (1991) Application of continuous relaxation time distributions to the fitting of data from model systems and excised tissue. *Magn Reson Med* **20**:214–227.
103. Meyers SM, Vavasour IM, Madler B, Harris T, Fu E, Li DK, Traboulsee AL, MacKay AL, Laule C (2013) Multicenter measurements of myelin water fraction and geometric mean T₂: intra- and intersite reproducibility. *J Magn Reson Imaging* **38**:1445–1453.
104. Miller DH, Thompson AJ, Filippi M (2003) Magnetic resonance studies of abnormalities in the normal appearing white matter and grey matter in multiple sclerosis. *J Neurol* **250**:1407–1419.
105. Minty EP, Bjarnason TA, Laule C, Mackay AL (2009) Myelin water measurement in the spinal cord. *Magn Reson Med* **61**:883–892.
106. Moll NM, Rietsch AM, Thomas S, Ransohoff AJ, Lee JC, Fox R, Chang A, Ransohoff RM, Fisher E (2011) Multiple sclerosis normal-appearing white matter: pathology-imaging correlations. *Ann Neurol* **70**:764–773.
107. Moore GR, Laule C, Mackay A, Leung E, Li DK, Zhao G, Traboulsee AL, Paty DW (2008) Dirty-appearing white matter in multiple sclerosis : preliminary observations of

- myelin phospholipid and axonal loss. *J Neurol* **255**:1802–1811.
108. Moore GRW (1998) Neuropathology and pathophysiology of the multiple sclerosis lesion. In: Mult Scler. Paty D, Ebers GC (eds), pp. 257–327. F.A. Davis: Philadelphia.
 109. Moore GRW (2003) MRI—clinical correlations: more than inflammation alone—what can MRI contribute to improve the understanding of pathological processes in MS. *J Neurol Sci* **206**:175–179.
 110. Moore GRW, Stadelmann-Nessler C (2015) Demyelinating diseases. In: Greenfield's Neuropathology, 9th edn. Love S, Budka H, Ironside JW, Perry A (eds.), pp. 1297–1412. Taylor and Francis (CRC Press): Boca Raton, FL.
 111. Moore GRW, Leung E, MacKay AL, Vavasour IM, Whittall KP, Cover KS, Li DK, Hashimoto SA, Oger J, Sprinkle TJ, Paty DW (2000) A pathology-MRI study of the short- T_2 component in formalin-fixed multiple sclerosis brain. *Neurology* **55**:1506–1510.
 112. Mottershead JP, Schmierer K, Clemence M, Thornton JS, Scaravilli F, Barker GJ, Tofts PS, Newcombe J, Cuzner ML, Ordidge RJ, McDonald WI, Miller DH (2003) High field MRI correlates of myelin content and axonal density in multiple sclerosis—a post-mortem study of the spinal cord. *J Neurol* **250**:1293–1301.
 113. Nam Y, Lee J, Hwang D, Kim DH (2015) Improved estimation of myelin water fraction using complex model fitting. *Neuroimage* **116**:214–221.
 114. Narayana PA, Wolinsky JS, Rao SB, He R, Mehta M (2004) Multicentre proton magnetic resonance spectroscopy imaging of primary progressive multiple sclerosis. *Mult Scler* **10**(Suppl 1):S73–S78.
 115. Nesbit GM, Forbes GS, Scheithauer BW, Okazaki H, Rodriguez M (1991) Multiple sclerosis: histopathologic and MR and/or CT correlation in 37 cases at biopsy and three cases at autopsy. *Radiology* **180**:467–474.
 116. Neu I, Woelk H (1982) Investigations of the lipid metabolism of the white matter in multiple sclerosis: changes in glycerophosphatides and lipid-splitting enzymes. *Neurochem Res* **7**:727–735.
 117. Newcombe J, Hawkins CP, Henderson CL, Patel HA, Woodroffe MN, Hayes GM, Cuzner ML, MacManus D, du Boulay EP, McDonald WI (1991) Histopathology of multiple sclerosis lesions detected by magnetic resonance imaging in unfixed postmortem central nervous system tissue. *Brain* **114**(Pt 2):1013–1023.
 118. Nguyen TD, Deh K, Monohan E, Pandya S, Spincemaille P, Raj A, Wang Y, Gauthier SA (2015) Feasibility and reproducibility of whole brain myelin water mapping in 4 minutes using fast acquisition with spiral trajectory and adiabatic T_2 prep (FAST- T_2) at 3T. *Magn Reson Med* **76**:456–465.
 119. Nguyen TD, Wisnieff C, Cooper MA, Kumar D, Raj A, Spincemaille P, Wang Y, Vartanian T, Gauthier SA (2012) T_2 prep three-dimensional spiral imaging with efficient whole brain coverage for myelin water quantification at 1.5 tesla. *Magn Reson Med* **67**:614–621.
 120. Nordengen K, Heuser C, Rinholm JE, Matalon R, Gundersen V (2015) Localisation of N-acetylaspartate in oligodendrocytes/myelin. *Brain Struct Funct* **220**:899–917.
 121. Odrobina EE, Lam TY, Pun T, Midha R, Stanisz GJ (2005) MR properties of excised neural tissue following experimentally induced demyelination. *NMR Biomed* **18**:277–284.
 122. Oh J, Han ET, Lee MC, Nelson SJ, Pelletier D (2007) Multislice brain myelin water fractions at 3T in multiple sclerosis. *J Neuroimaging* **17**:156–163.
 123. Oh J, Han ET, Pelletier D, Nelson SJ (2006) Measurement of *in vivo* multi-component T_2 relaxation times for brain tissue using multi-slice T_2 prep at 1.5 and 3 T. *Magn Reson Imaging* **24**:33–43. Epub 2005 Dec 19.
 124. Oh SH, Bilello M, Schindler M, Markowitz CE, Detre JA, Lee J (2013) Direct visualization of short transverse relaxation time component (ViSTa). *Neuroimage* **83**:485–492.
 125. Ormerod IE, Miller DH, McDonald WI, du Boulay EP, Rudge P, Kendall BE, Moseley IF, Johnson G, Tofts PS, Halliday AM *et al* (1987) The role of NMR imaging in the assessment of multiple sclerosis and isolated neurological lesions. A quantitative study. *Brain* **110**(Pt 6):1579–1616.
 126. Papanikolaou N, Papadaki E, Karampekios S, Spilioti M, Maris T, Prassopoulos P, Gourtsoyannis N (2004) T_2 relaxation time analysis in patients with multiple sclerosis: correlation with magnetization transfer ratio. *Eur Radiol* **14**:115–122.
 127. Paty DW, Moore GRW (1998) Magnetic resonance imaging changes as living pathology in multiple sclerosis. In: Mult Scler. Paty DW, Ebers GC (eds.), pp. 328–369. F.A. Davis: Philadelphia.
 128. Plumb J, McQuaid S, Mirakhor M, Kirk J (2002) Abnormal endothelial tight junctions in active lesions and normal-appearing white matter in multiple sclerosis. *Brain Pathol* **12**:154–169.
 129. Prasloski T, Madler B, Xiang QS, MacKay A, Jones C (2012) Applications of stimulated echo correction to multicomponent T_2 analysis. *Magn Reson Med* **67**:1803–1814.
 130. Prasloski T, Rauscher A, MacKay AL, Hodgson M, Vavasour IM, Laule C, Madler B (2012) Rapid whole cerebrum myelin water imaging using a 3D GRASE sequence. *Neuroimage* **63**:533–539.
 131. Prineas JW, McDonald WI, Franklin RJM (2002) Demyelinating diseases. In: Greenfield's Neuropathology. Graham DI, Lantos PL (eds.), pp. 471–550. Arnold: London.
 132. Pun TW, Odrobina E, Xu QG, Lam TY, Munro CA, Midha R, Stanisz GJ (2005) Histological and magnetic resonance analysis of sciatic nerves in the tellurium model of neuropathy. *J Peripher Nerv Syst* **10**:38–46.
 133. Raine CS (1997) Demyelinating disease. In: *Textbook of Neuropathology*. Davis RL, Robertson DM (eds.), pp. 627–714. Williams & Wilkins: Baltimore.
 134. Raj A, Pandya S, Shen X, LoCastro E, Nguyen TD, Gauthier SA (2014) Multi-compartment T_2 relaxometry using a spatially constrained multi-Gaussian model. *PLoS ONE* **9**:e98391.
 135. Riekkinen PJ, Rinne UK, Arstila AU (1972) Neurochemical and morphological studies on demyelination in multiple sclerosis with special reference to etiological aspects. *Z Neurol* **203**:91–104.
 136. Rinne UK, Riekkinen P, Arstila AU (1972) Biochemical and electron microscopic alterations in the white matter outside demyelinated plaques in multiple sclerosis. In: *Progress in Multiple Sclerosis*. Lubowitz U (ed), pp. 76–98. Academic Press: New York.
 137. Robson MD, Gatehouse PD, Bydder M, Bydder GM (2003) Magnetic resonance: an introduction to ultrashort TE (UTE) imaging. *J Comput Assist Tomogr* **27**:825–846.

138. Rooney WD, Johnson G, Li X, Cohen ER, Kim SG, Ugurbil K, Springer CS Jr (2007) Magnetic field and tissue dependencies of human brain longitudinal $^1\text{H}_2\text{O}$ relaxation *in vivo*. *Magn Reson Med* **57**:308–318.
139. Ropele S, Strasser-Fuchs S, Augustin M, Stollberger R, Enzinger C, Hartung HP, Fazekas F (2000) A comparison of magnetization transfer ratio, magnetization transfer rate, and the native relaxation time of water protons related to relapsing-remitting multiple sclerosis. *AJNR Am J Neuroradiol* **21**:1885–1891.
140. Rovira A, de Stefano N (2016) MRI monitoring of spinal cord changes in patients with multiple sclerosis. *Curr Opin Neurol* **29**:445–452.
141. Salthouse T (1962) Luxol fast blue ARN: a new solvent azo dye with improved staining qualities for myelin and phospholipids. *Staining Technol* **37**:313–316.
142. Sati P, van Gelderen P, Silva AC, Reich DS, Merkle H, de Zwart JA, Duyn JH (2013) Micro-compartment specific T_2^* relaxation in the brain. *Neuroimage* **77**:268–278.
143. Schilling KG, Janve V, Gao Y, Stepniewska I, Landman BA, Anderson AW (2018) Histological validation of diffusion MRI fiber orientation distributions and dispersion. *Neuroimage* **165**:200–221.
144. Schmierer K, Scaravilli F, Altmann DR, Barker GJ, Miller DH (2004) Magnetization transfer ratio and myelin in postmortem multiple sclerosis brain. *Ann Neurol* **56**:407–415.
145. Seewann A, Vrenken H, van der Valk P, Blezer EL, Knol DL, Castelijns JA, Polman CH, Pouwels PJ, Barkhof F, Geurts JJ (2009) Diffusely abnormal white matter in chronic multiple sclerosis: imaging and histopathologic analysis. *Arch Neurol* **66**:601–609.
146. Segarra J (1970) Histological and histochemical staining methods. In: *Neuropathology Methods and Diagnosis*. Teduchi C (ed), pp. 233–269. Little, Brown and Company: Boston.
147. Shen X, Nguyen TD, Gauthier SA, Raj A (2013) Robust myelin quantitative imaging from multi-echo T_2 MRI using edge preserving spatial priors. *Med Image Comput Comput-Assisted Intervention: MICCAI Int Conf Med Image Comput Comput-Assisted Intervention* **16**(Pt 1):622–630.
148. Sheth V, Shao H, Chen J, Vandenberg S, Corey-Bloom J, Bydder GM, Du J (2016) Magnetic resonance imaging of myelin using ultrashort Echo time (UTE) pulse sequences: phantom, specimen, volunteer and multiple sclerosis patient studies. *Neuroimage* **136**:37–44.
149. Simon JH, Kinkel RP, Jacobs L, Bub L, Simonian N (2000) A Wallerian degeneration pattern in patients at risk for MS. *Neurology* **54**:1155–1160.
150. Sinclair C, Mirakhur M, Kirk J, Farrell M, McQuaid S (2005) Up-regulation of osteopontin and alphaBeta-crystallin in the normal-appearing white matter of multiple sclerosis: an immunohistochemical study utilizing tissue microarrays. *Neuropathol Appl Neurobiol* **31**:292–303.
151. Sirrs SM, Laule C, Maedler B, Brief EE, Tahir SA, Bishop C, MacKay AL (2007) Normal appearing white matter in subjects with phenylketonuria: water content, myelin water fraction, and metabolite concentrations. *Radiology* **242**:236–243.
152. Smith KJ, McDonald WI (1999) The pathophysiology of multiple sclerosis: the mechanisms underlying the production of symptoms and the natural history of the disease. *Philos Trans R Soc London B Biol Sci* **354**:1649–1673.
153. Sobel RA (2005) Ephrin A receptors and ligands in lesions and normal-appearing white matter in multiple sclerosis. *Brain Pathol* **15**:35–45.
154. Sobel RA, Ahmed AS (2001) White matter extracellular matrix chondroitin sulfate/dermatan sulfate proteoglycans in multiple sclerosis. *J Neuropathol Exp Neurol* **60**:1198–1207.
155. Song SK, Yoshino J, Le TQ, Lin SJ, Sun SW, Cross AH, Armstrong RC (2005) Demyelination increases radial diffusivity in corpus callosum of mouse brain. *Neuroimage* **26**:132–140.
156. Stadelmann C, Albert M, Wegner C, Bruck W (2008) Cortical pathology in multiple sclerosis. *Curr Opin Neurol* **21**:229–234.
157. Stanisz GJ, Henkelman RM (1998) Diffusional anisotropy of T_2 components in bovine optic nerve. *Magn Reson Med* **40**:405–410.
158. Stanisz GJ, Webb S, Munro CA, Pun T, Midha R (2004) MR properties of excised neural tissue following experimentally induced neuroinflammation. *Magn Reson Med* **51**:473–479.
159. Stewart WA, Hall LD, Berry K, Churg A, Oger J, Hashimoto SA, Paty DW (1986) Magnetic resonance imaging (MRI) in multiple sclerosis (MS): pathological correlation in eight cases. *Neurology* **36**(suppl 1):320.
160. Stewart WA, Hall LD, Berry K, Paty DW (1984) Correlation between NMR scan and brain slice data in multiple sclerosis. *Lancet* **2**:412.
161. Stewart WA, MacKay AL, Whittall KP, Moore GR, Paty DW (1993) Spin-spin relaxation in experimental allergic encephalomyelitis. Analysis of CPMG data using a non-linear least squares method and linear inverse theory. *Magn Reson Med* **29**:767–775.
162. Stüber C, Morawski M, Schafer A, Labadie C, Wahnert M, Leuze C, Streicher M, Barapatre N, Reimann K, Geyer S, Spemann D, Turner R (2014) Myelin and iron concentration in the human brain: a quantitative study of MRI contrast. *Neuroimage* **93**(Pt 1):95–106.
163. Suzuki K, Kamoshita S, Eto Y, Tourtellotte WW, Gonatas JO (1973) Myelin in multiple sclerosis. Composition of myelin from normal-appearing white matter. *Arch of Neurol* **28**:293–297.
164. Tallantyre EC, Bo L, Al-Rawashdeh O, Owens T, Polman CH, Lowe JS, Evangelou N (2010) Clinico-pathological evidence that axonal loss underlies disability in progressive multiple sclerosis. *Mult Scler* **16**:406–411.
165. Tofts PS (2003) *Quantitative MRI of the Brain : Measuring Changes Caused by Disease*. Wiley: Chichester, West Sussex; Hoboken, NJ.
166. Tozer DJ, Davies GR, Altmann DR, Miller DH, Tofts PS (2005) Correlation of apparent myelin measures obtained in multiple sclerosis patients and controls from magnetization transfer and multicompartamental T_2 analysis. *Magn Reson Med* **53**:1415–1422.
167. Trapp BD, Peterson J, Ransohoff RM, Rudick R, Mork S, Bo L (1998) Axonal transection in the lesions of multiple sclerosis. *N Engl J Med* **338**:278–285.
168. Valentine HL, Does MD, Marshall V, Tonkin EG, Valentine WM (2007) Multicomponent T_2 analysis of dithiocarbamate-mediated peripheral nerve demyelination. *Neurotoxicology* **28**:645–654.
169. van Walderveen MA, Kamphorst W, Scheltens P, van Waesberghe JH, Ravid R, Valk J, Polman CH, Barkhof F (1998) Histopathologic correlate of hypointense lesions on

- T_1 -weighted spin-echo MRI in multiple sclerosis. *Neurology* **50**:1282–1288.
170. van Walderveen MA, van Schijndel RA, Pouwels PJ, Polman CH, Barkhof F (2003) Multislice T_1 relaxation time measurements in the brain using IR-EPI: reproducibility, normal values, and histogram analysis in patients with multiple sclerosis. *J Magn Reson Imaging* **18**:656–664.
 171. Vargas WS, Monohan E, Pandya S, Raj A, Vartanian T, Nguyen TD, Hurtado Rua SM, Gauthier SA (2015) Measuring longitudinal myelin water fraction in new multiple sclerosis lesions. *Neuroimage Clin* **9**:369–375.
 172. Varma G, Duhamel G, de Bazelaire C, Alsop DC (2015) Magnetization transfer from inhomogeneously broadened lines: a potential marker for myelin. *Magn Reson Med* **73**:614–622.
 173. Varma G, Girard OM, Prevost VH, Grant AK, Duhamel G, Alsop DC (2015) Interpretation of magnetization transfer from inhomogeneously broadened lines (ihMT) in tissues as a dipolar order effect within motion restricted molecules. *J Magn Reson* **260**:67–76.
 174. Vavasour IM, Clark CM, Li DK, Mackay AL (2006) Reproducibility and reliability of MR measurements in white matter: clinical implications. *Neuroimage* **32**:637–642. [Epub 2006 May 3].
 175. Vavasour IM, Huijskens SC, Li DK, Traboulsee AL, Madler B, Kolind SH, Rauscher A, Moore GW, MacKay AL, Laule C (2017) Global loss of myelin water over 5 years in multiple sclerosis normal-appearing white matter. *Mult Scler*. [Epub ahead of print].
 176. Vavasour IM, Laule C, Li DK, Oger J, Moore GR, Traboulsee A, MacKay AL (2009) Longitudinal changes in myelin water fraction in two MS patients with active disease. *J Neurol Sci* **276**:49–53.
 177. Vavasour IM, Laule C, Li DK, Traboulsee AL, MacKay AL (2011) Is the magnetization transfer ratio a marker for myelin in multiple sclerosis? *J Magn Reson Imaging* **33**:713–718.
 178. Vavasour IM, Li DK, Laule C, Traboulsee AL, Moore GR, Mackay AL (2007) Multi-parametric MR assessment of $T(1)$ black holes in multiple sclerosis: evidence that myelin loss is not greater in hypointense versus isointense $T(1)$ lesions. *J Neurol* **254**:1653–1659.
 179. Vavasour IM, Tam R, Li DK, Laule C, Taylor C, Kolind SH, MacKay AL, Javed A, Traboulsee A (2018) A 24-month advanced magnetic resonance imaging study of multiple sclerosis patients treated with alemtuzumab. *Mult Scler*. [Epub ahead of print].
 180. Vavasour IM, Whittall KP, MacKay AL, Li DK, Vorobeychik G, Paty DW (1998) A comparison between magnetization transfer ratios and myelin water percentages in normals and multiple sclerosis patients. *Magn Reson Med* **40**:763–768.
 181. Vercellino M, Masera S, Lorenzatti M, Condello C, Merola A, Mattioda A, Tribolo A, Capello E, Mancardi GL, Mutani R, Giordana MT, Cavalla P (2009) Demyelination, inflammation, and neurodegeneration in multiple sclerosis deep gray matter. *J Neuropathol Exp Neurol* **68**:489–502.
 182. Vos CM, Geurts JJ, Montagne L, van Haastert ES, Bo L, van der Valk P, Barkhof F, de Vries HE (2005) Blood-brain barrier alterations in both focal and diffuse abnormalities on postmortem MRI in multiple sclerosis. *Neurobiol Dis* **20**:953–960.
 183. Vrenken H, Seewann A, Knol DL, Polman CH, Barkhof F, Geurts JJ (2010) Diffusely abnormal white matter in progressive multiple sclerosis: *in vivo* quantitative MR imaging characterization and comparison between disease types. *AJNR Am J Neuroradiol* **31**:541–548.
 184. Wang X, Cusick MF, Wang Y, Sun P, Libbey JE, Trinkaus K, Fujinami RS, Song SK (2014) Diffusion basis spectrum imaging detects and distinguishes coexisting subclinical inflammation, demyelination and axonal injury in experimental autoimmune encephalomyelitis mice. *NMR Biomed* **27**:843–852.
 185. Webb S, Munro CA, Midha R, Stanisz GJ (2003) Is multicomponent T_2 a good measure of myelin content in peripheral nerve? *Magn Reson Med* **49**:638–645.
 186. Weil A (1928) A rapid method for staining myelin sheaths. *Arch Neurol Psych* **20**:392–393.
 187. Werring DJ, Clark CA, Droogan AG, Barker GJ, Miller DH, Thompson AJ (2001) Water diffusion is elevated in widespread regions of normal-appearing white matter in multiple sclerosis and correlates with diffusion in focal lesions. *Mult Scler* **7**:83–89.
 188. Whittall KP, MacKay AL (1989) Quantitative interpretation of nmr relaxation data. *J Magn Reson* **84**:134–152.
 189. Whittall KP, MacKay AL, Graeb DA, Nugent RA, Li DK, Paty DW (1997) *In vivo* measurement of T_2 distributions and water contents in normal human brain. *Magn Reson Med* **37**:34–43.
 190. Wilhelm MJ, Ong HH, Wehrli SL, Li C, Tsai PH, Hackney DB, Wehrli FW (2012) Direct magnetic resonance detection of myelin and prospects for quantitative imaging of myelin density. *Proc Natl Acad Sci USA* **109**:9605–9610.
 191. Wolff SD, Balaban RS (1989) Magnetization transfer contrast (MTC) and tissue water proton relaxation *in vivo*. *Magn Reson Med* **10**:135–144.
 192. Wright AD, Jarrett M, Vavasour I, Shahinfard E, Kolind S, van Donkelaar P, Taunton J, Li D, Rauscher A (2016) Myelin water fraction is transiently reduced after a single mild traumatic brain injury—a prospective cohort study in collegiate hockey players. *PLoS ONE* **11**:e0150215.
 193. Wu Y, Alexander AL, Fleming JO, Duncan ID, Field AS (2006) Myelin water fraction in human cervical spinal cord *in vivo*. *J Comput Assist Tomogr* **30**:304–306.
 194. Yanagihara T, Cumings JN (1969) Alterations of phospholipids, particularly plasmalogens, in the demyelination of multiple sclerosis as compared with that of cerebral oedema. *Brain* **92**:59–70.
 195. Yu RK, Ueno K, Glaser GH, Tourtellotte WW (1982) Lipid and protein alterations of spinal cord and cord myelin of multiple sclerosis. *J Neurochem* **39**:464–477.
 196. Zhao G, Li DKB, Cheng Y, Paty DW, UBC MS/MRI Research Group, PRISMS Study Group (2003) Possible prognostic significance of dirty-appearing white matter on MRI in multiple sclerosis. *Mult Scler* **9**(Suppl 1):S61.
 197. Zhao GJ, Li DKB, Cheng Y, Wang XY, Paty DW, The UBC MS/MRI Research Group, PRISMS Study Group (2000) MRI dirty-appearing white matter in MS. *Neurology* **54**(suppl 3):A121.